https://doi.org/10.48048/tis.2025.9476

In-Situ Synthesis of AgNPs using *Boesenbergia Rotunda* L. Extract as Reducing Agent Development of Antibacterial and UV Protective Muslin Fabrics

Nipaporn Pimsin[1], Jirapad Janshongsawang[1], Saksit Chanthai[1], Montakarn Thongsom[3], Prawit Nuengmatcha[2,4] and Paweena Porrawatkul[2,*]

[1]Materials Chemistry Research Center, Department of Chemistry and Center of Excellence for Innovation in Chemistry, Faculty of Science, Khon Kaen University, Khon Kaen 40002, Thailand
[2]Center of Excellence in Nanomaterials Chemistry, Department of Chemistry, Faculty of Science and Technology, Nakhon Si Thammarat Rajabhat University, Nakhon Si Thammarat 80280, Thailand
[3]Department of Biology, Faculty of Science and Technology, Nakhon Si Thammarat Rajabhat University, Nakhon Si Thammarat 80280, Thailand
[4]Department of Creative innovation in Science and Technology, Faculty of Science and Technology, Nakhon Si Thammarat Rajabhat University, Nakhon Si Thammarat 80280, Thailand

([*]Corresponding author's e-mail: paweena_por@nstru.ac.th)

Received: 9 December 2024, Revised: 28 December 2024, Accepted: 4 January 2025, Published: 20 February 2025

Abstract

Muslin fabrics functionalized with silver nanoparticles (AgNPs) need to be produced via green synthesis to protect against ultraviolet (UV) radiation and antibacterial activity. In this study, we performed the green synthesis of AgNPs functionalized with fingerroot (*Boesenbergia rotunda* (L.) Mansf.) extract. The main bioactive component of fingerroot was investigated via GC-MS. The primary ingredient in fingerroot, pinostrobin, was shown to be the most prevalent, based on the GC-MS data. An eco-friendly approach involves obtaining such textile materials by AgNP synthesis directly (*in situ*) on muslin fabrics. The chemical linkages of colloidal AgNPs to the cellulosic structure were characterized and confirmed by FTIR, SEM, and EDX analyses. Compared to uncoated muslin fabric, AgNP-coated fabric provides excellent protection, with a UV protection factor (UPF) value of 43.30 and Insufficient protection, with a UPF value of 6.42. The antibacterial activity of AgNP-coated fabric was investigated, revealing greater inhibitory effects against *Staphylococcus aureus* (gram-positive) and *Escherichia coli* (gram-negative) microbial strains. A wash durability test was also performed on the treated fabric, and the findings showed that it could maintain strong antibacterial activity for up to 10 wash cycles. All of these findings pointed to the AgNPs produced in this study as a potentially useful ingredient for creating fabrics with strong antibacterial and UV protection properties.

Keywords: Antimicrobial, Fingerroot, Muslin fabric, Silver nanoparticles

Introduction

Textiles protect human skin from harmful substances, such as viruses, bacteria, and contaminated air. Muslin is a thin cotton fabric with a plain weave. It is popular for its fine, silky texture and has widespread applications because of its breathability and versatility. Owing to its superior qualities, including elasticity, softness, water absorption, and breathability, cotton fabric is highly popular among consumers [1]. However, cotton textiles encourage bacterial growth [2,3], which decreases their wearability because of certain health hazards [4-6]. Several surface modification procedures can improve the cotton fabric and impart the prepared materials with antibacterial and fire-resistance properties, along with high durability after washing [7,8]. One such method involves the use of metal oxide nanoparticles, such as zinc oxide and silver

nanoparticles (AgNPs) [9]. AgNPs are a common choice among all noble metal nanoparticles used to combat diseases because of their superior and broad-spectrum antibacterial activity against various strains [10,11]. As a result, microbial cells find it extremely challenging to undergo several concurrent gene changes in response to AgNP-mediated therapies.

Various methods are available for synthesizing AgNPs, including chemical reduction, sonochemical, microwave-assisted, and green synthesis techniques [12-14]. The green synthesis approach for producing nanoparticles has attracted much interest as an alternative strategy to conventional methods because of its low cost and used natural plant resources as active phytocompounds that serve as capping and reducing agents [15-17]. Additionally, this method uses renewable materials, operates in ambient circumstances, uses little energy, and has little effect on the environment, it promotes sustainability in general [18]. In addition, synthetic stabilizers and reducers offer better reproducibility and scalability at an industrial level but involve higher costs and environmental concerns. However, plant extracts economically attractive and environmentally friendly for small- to medium-scale synthesis, but challenges include variability and scalability.

Fingerroot (*Boesenbergia rotunda* (L.) Mansf.), or ginseng of Thailand, is a herbal plant well-known for its immune activities; it consists of several bioactive compounds [19]. Fingerroot was used as a reducing agent for synthesizing nanomaterials; for example, fingerroot was used as a reducing agent to synthesize zinc oxide (ZnO) thin films using the dip coating technique [20], and it was used as a reducing and capping agent to synthesize AgNPs used as ingredient of acrylic resin denture base material [21]. AgNP-coated muslin is a promising material for protective and medical textile applications because of this new biochemical finding, which shows how fingerroot extract might improve the textile's functional qualities. Innovative and sustainable textile solutions are becoming more and more necessary to meet these issues.

The objective of this work is to create multipurpose, environmentally friendly textiles by utilizing greenly synthesized silver nanoparticles (AgNPs). We investigated the ability of *Boesenbergia rotunda* (L.) Mansf. (fingerroot) to act as a reducing agent for the formation of AgNPs directly on muslin fabrics. The main chemical composition of fingerroot was studied by gas chromatography-mass spectrometry (GC-MS). The findings showed that cellulosic textiles provide strong protection against UV radiation as well as *Escherichia coli* and *Staphylococcus aureus*. This study supports SDGs 6: Clean Water and Sanitation and SDGs 12: Responsible Consumption and Production by making use of natural resources and reducing the usage of hazardous chemicals [22]. Additionally, in line with SDGs 3: Good Health and Well-Being, the new textiles improved antibacterial and UV-protective qualities might benefit public health and well-being.

Materials and methods

Materials

All reagents used in the present work were of analytical grade and were purchased from Merck. The nutrient agar for bacterial culture, the Mueller–Hinton broth, and the antimicrobial activity agar was purchased from Hi-Media (Mumbai, India). muslin fabric was purchased from Khon Khen province, Thailand. Distilled water was used in the experiments.

Preparation of the fingerroot extract

Fresh fingerroot (50 g) was selected and washed to remove the residue. The samples were cut into small pieces and blended in a blender. Fresh fingerroot samples were added to 100 mL of 80 % ethanol at a ratio of 1:2 for 15 min. Next, the fingerroot extract was filtered through a funnel and filter paper. The filtrate of the fingerroot extract was stored at 4 °C until further use. The molecular composition and structure of the extract were determined via FTIR spectroscopy (TENSOR27 system Fourier transform infrared spectrometer (Bruker, Germany)), and the chemical composition was analyzed via GC-MS.

GC-MS analysis of the fingerroot extract

Gas chromatography-mass spectrometry (GC-MS) analysis of the fingerroot extract was performed using triple quadrupole GC-MS/MS (model: Agilent 7000C GC-MS Triple Quad). The equipment had a column with dimensions of 30 mm×0.25 mm i.d.×0.25 μm film. The carrier gas used was He (flow rate: 1.0 mL/min). The oven temperature was set as follows, with

the injector running at 270 °C: 3 min at 50 °C, followed by an increase to 300 °C in 5 min. The constituents were identified by comparing the obtained spectra to those present in a virtual library (Wiley 12th/NIST 2020) attached to the GC-MS instrument.

Conditional studies for the synthesis of AgNPs using fingerroot extract

For the experiment, 10 mL of the fingerroot extract was added dropwise to 50 mL of a 1 mM $AgNO_3$ aqueous solution. The solution (pH adjusted to 10) was heated at 85 °C for 1 h under ultrasonic irradiation. The optimization experiment involved adding different amounts (0.5, 1.0, 2.0, 5.0, 7.5 and 10 mL) of fingerroot extract. The different concentrations (1 µM, 10 µM, 1 mM, 5 mM, and 10 mM) of silver nitrate hexahydrate were optimized. The AgNP-fingerroot solution obtained was stored at 4 °C until further use.

***In-situ* synthesis of AgNPs on muslin fabric**

The in situ AgNP-fingerroot coating of muslin fabric was investigated. A muslin fabric (5×5 cm) was immersed in a solution of 1 mM $AgNO_3$ in a 250 mL Erlenmeyer flask under ultrasonic irradiation at 85 °C. Then, 50 mL of $AgNO_3$ (1 mM) and 5 mL of buffer (pH 10) were added, and the mixture was sonicated for 3 h. The mixture was subsequently incubated for 24 h at room temperature in the dark. The coated fabric was removed from the mixture and dried at 70 °C for 10 min. The same procedure was used to prepare the uncoated muslin fabric in a 250 mL Erlenmeyer flask at 85 °C with ultrasonic irradiation, but no further reaction chemicals were used.

Characterization of the biosynthesized AgNPs

The surface morphology of the biosynthesized AgNPs nanoparticles was examined by scanning electron microscopy (SEM, Hitachi S-3000N scanning electron microscope, Hitachi Co. Ltd., Japan), and the elemental composition of the materials was analyzed via energy-dispersive X-ray spectroscopy (EDX, Hitachi S-3000 N). Additionally, the absorbance spectra of the AgNPs were observed in the 200 - 800 nm wavelength range using an Agilent 8453 UV-visible spectrophotometer (Germany). The particle size of synthesized AgNPs survey by nanoparticle analyzer (nanoPartica SZ-100V2 Series, HORIBA, Ltd. Japan)

Antimicrobial activity

The antibacterial activities of the fingerroot extract, AgNPs, and modified muslin fabric against *S. aureus* and *E. coli* were evaluated using the agar well diffusion method. A sterile cotton swab was used to spread the bacterial culture evenly across the nutrient agar plate. The diameter of the inhibition zone surrounding the sample was measured and compared to that around the negative control after incubation at 37 °C for 24 h. The durability of the antibacterial activity after washing was determined by treating the modified fabrics with 1 g/L laundry detergent at 35 °C for 20 min, and then, the activity was measured.

UV protection property analysis

UV-Vis spectroscopy was performed to assess how the treated and untreated cotton fabrics responded to UV radiation. The efficiency of UV shielding was assessed by measuring the absorption and transmission of UV. Using transmission statistics and pertinent calculations, the ultraviolet protection factor (UPF) and percentage of UV transmission were determined. The mean percentage transmission in the UV band (280 - 400 nm) was used to compute the UPF. This was performed by dividing the average effective irradiance for skin by the average UV irradiation for the skin covered by the fabric under evaluation (AATCC Test Method 183-2004) [23].

$$UPF = \frac{\sum_{280}^{400} E_\lambda S_\lambda \Delta_\lambda}{\sum_{280}^{400} E_\lambda S_\lambda T_\lambda \Delta_\lambda}$$

Here, E_λ represents the relative erythemal spectral effectiveness, S_λ represents the solar spectral irradiance in W m^{-2} nm^{-1}, and T_λ represents the UV spectrometric spectral transmission specimen.

Results and discussion

GC-MS analysis of the fingerroot extract

The GC-MS technique was used to determine the composition of the fingerroot extract, and about 16 bioactive compounds were identified. The molecular

formula, molecular weight, composition (%), and retention time of these compounds were determined from their peak areas. The GC-MS spectrum (**Figure 1**) of the fingerroot extract showed that the major compound was pinostrobin. Pinostrobin, a major constituent of Thai fingerroot [24], was found at the highest concentration (100 %), followed by camphor (35.64 %), beta-ocimene (31.30 %), geranol (25.59 %), eucalyptol (18.31 %), pinocembrin (16.29 %), hexadecanoic acid, ethyl ester (6.71 %), 2-propenoic acid, 3-phenyl- methyl ester (6.62 %), bicyclo [2,2,1]heptane, 2,2-dimethyl-3-methylene (4.68 %), 3-carene (3.48 %), ethyl oleate (2.89 %), linoleic acid ethyl ester (2.63 %), D-limonene (2.04 %), and other compounds present in trace amounts. However, the minor bioactive compounds in fingerroot extract might contribute to nanoparticle formation or stabilization. Compounds such as flavonoids, phenolics, and alkaloids, even in small amounts, can act as reducing agents, converting metal ions to nanoparticles. Additionally, these compounds often possess functional groups like hydroxyl or carboxyl, which can interact with the nanoparticle surface, stabilizing them by preventing aggregation.

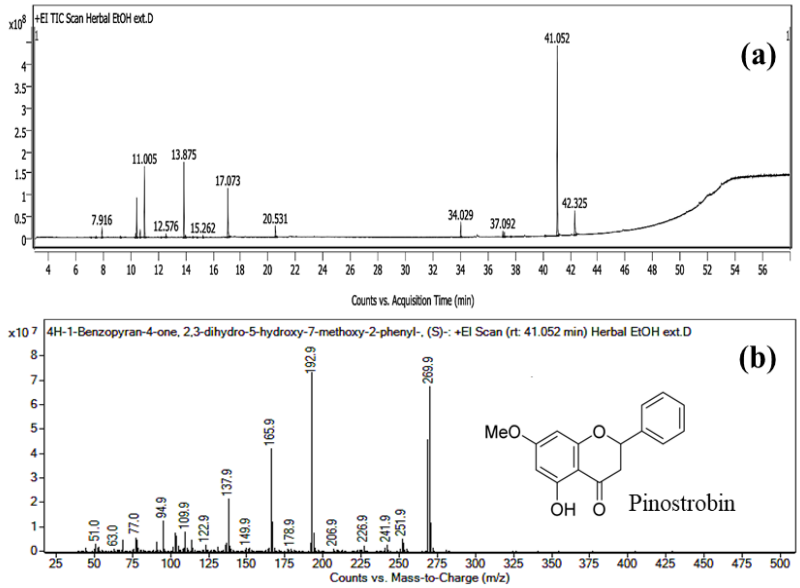

Figure 1 (a) GC-MS chromatogram of the ethanolic extract of fingerroot and (b) typical mass fractions and chemical structure of pinostrobin found in the fingerroot extract.

Biosynthesis of AgNPs using fingerroot extract

UV-Visible analysis

The as-synthesized AgNPs were studied using simple UV-visible spectroscopy. The absorption spectra of the synthesized AgNPs, along with the absorption spectrum of the fingerroot extract, are shown in **Figure 2**. The reduction of Ag^+ ions by the fingerroot extract was described by visual changes in the color of the solution from yellow to deep brown (**Figure 2(a)**) owing to surface plasmon vibrations in the AgNPs [25]. To investigate the interaction and reduction of Ag^+ ions by the extract, the absorption spectrum of the pure extract was recorded. As shown in **Figure 2(b)**, the narrow peak at about 290 nm obtained from the extract was attributed mainly to the UV absorption of polyphenols, and the peak at about 416 nm was the characteristic band of the AgNPs due to surface plasmon resonance (SPR).

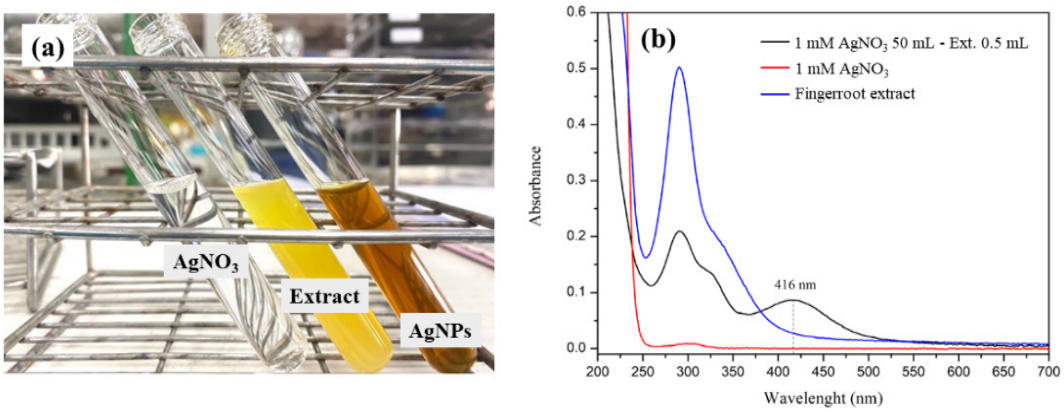

Figure 2 (a) Appearance of synthesized AgNPs, the fingerroot extract, and starting $AgNO_3$. (b) UV spectrum of the fingerroot extract, starting $AgNO_3$, and synthesized AgNPs.

The effects of different parameters on the synthesis of AgNPs

Effect of Ag^+ concentration

The effects of 1 µM, 10 µM, 1 mM, 5 mM, and 10 mM Ag^+ at pH 10 were assessed, and the respective absorbance values determined by UV-visible spectrophotometry are shown in **Figure 3(a)**. The maximum absorbance was obtained at 5 mM with SPR 416 nm. Increasing the Ag^+ concentration to 10 mM led to a decrease in the absorbance, which indicated that at higher concentrations, the yield of nanoparticles decreased. As the concentration increased to 10 mM, the SPR peak shifted toward shorter wavelengths. The decrease in absorbance caused by an increase in precipitation and particle aggregation suggested an increase in particle destabilization [26]. Based on these results, 5 mM $AgNO_3$ was used to further investigate the amount of fingerroot extract.

Effect of the amount of fingerroot extract

Different quantities of the extract (0.5, 1.0, 2.0, 5.0, 7.5 and 10 mL) with a fixed amount of silver nitrate solution (50 mL, 5 mM) were used to synthesize AgNPs at pH 10. The maximum absorbance was obtained at 5 mM with SPR at 416 nm (**Figure 3(b)**). Increasing the Ag^+ concentration to 10 mM led to a decrease in the absorbance, which indicated that at higher concentrations, the yield of nanoparticles decreased. When the quantity of fingerroot extracted increased from 0.5 to 5 mL, the absorbance of the AgNPs at 416 nm increased. The maximum absorbance of the reducing agent was 5 mL. However, the quantity of fingerroot extract above 5 mL (7.5 and 10 mL) decreased due to aggregation [9]. Therefore, 5 mL of the fingerroot extract was used for the *in-situ* synthesis of AgNPs on muslin fabric fibers.

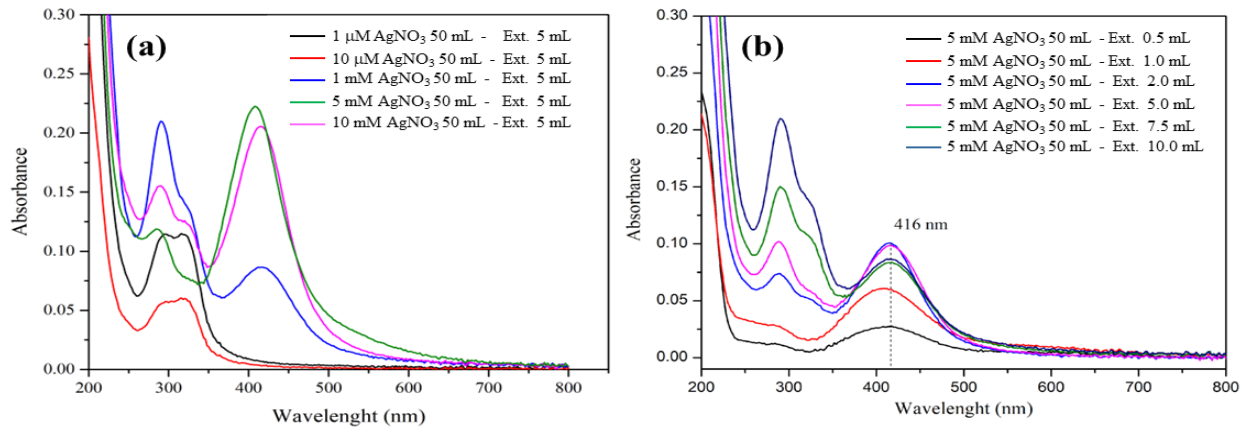

Figure 3 UV-Vis Spectrum of (a) Effect of Ag^+ concentration on AgNP-fingerroot. (b) Effect of the amount of fingerroot extract.

Morphological studies of biosynthesized AgNPs

The morphology of the synthesized AgNPs was characterized by SEM analysis. The SEM images of the spherical shape of the AgNPs at 10 kV are shown in **Figure 4(a)**. **Figure 4(b)** showed the particle-size distribution of *in-situ* synthesized AgNPs sample revealed that the particles ranged in size from 11 to 19 nm, with an average size of 15 nm. The biosynthesized AgNPs are spherical, evenly dispersed, and firmly attached to the surface of the muslin fabric, according to the SEM examination. These features guarantee improved functional qualities like antibacterial activity and UV protection for the treated fabric, confirming the efficacy of the fingerroot-mediated synthesis process. The elemental compositions of the samples were confirmed by EDX. The EDX analysis of the AgNPs synthesized with fingerroot extract as the reducing agent showed a composition of C (54.7 %), O (21.4 %), and Ag (23.9 %) (**Figure 4(c)**).

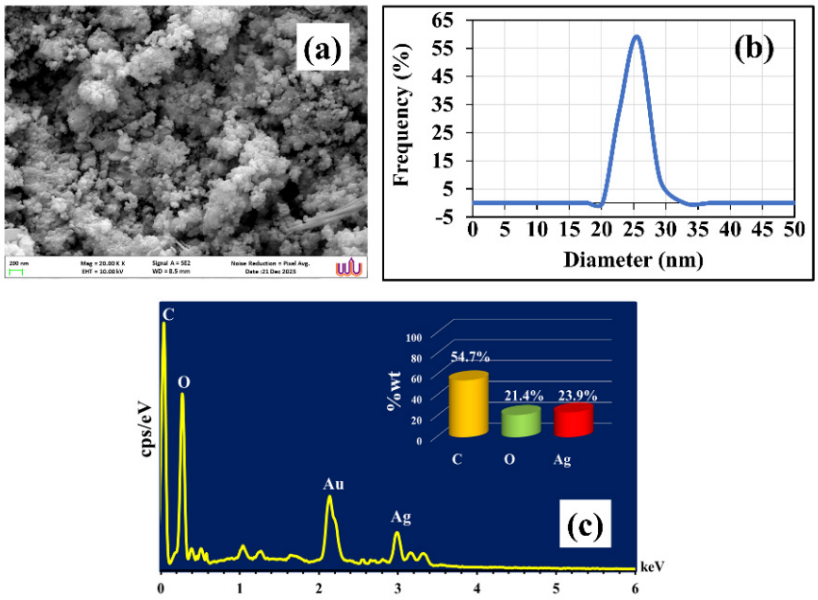

Figure 4 (a) SEM image of the AgNPs at 10 kV, (b) particle size of *in-situ* AgNPs and (c) EDX spectra of the AgNPs.

FT-IR analysis

FTIR spectra of the starting material, the fingerroot extract and biosynthesized silver nanoparticles are shown in **Figure 5**. The $AgNO_3$ sample analysis (**Figure 5(a)**) shows peaks as follows, 1,265 cm^{-1} related to the N-O of the nitrate and 1,757 cm^{-1} of amino groups [27]. The FTIR spectra of fingerroot extract, depicted in **Figure 5(b)**, presented the C–H stretching vibration of the $–CH_3$ group at approximately 2,927 cm^{-1}. The broad spectral peak at 3,267 cm^{-1} represented the O–H stretching of alcohols [28]. The sharp peak at 1,620 cm^{-1} corresponded to the C=O functional groups. The FTIR spectrum of AgNPs exhibited decreased O–H and C–O stretching intensity (**Figure 5(c)**), the C–O stretching peak at 1,393 cm^{-1}, and a broad peak for O–H stretching at 3,227 cm^{-1}, indicating the oxidation of the C=O group to the –COOH group [29]. The FTIR data indicate that the creation of silver nanoparticles was attributed to the O–H and C=O groups in the fingerroot extract, namely, the O–H groups in phenolic compounds, flavonoids (e.g., pinostrobin), and other phytochemicals present in fingerroot that act as reducing agents. The O–H groups donate electrons to silver ions (Ag^+), reducing them to elemental silver (Ag^0), which forms the basis for nanoparticle nucleation. A decrease in the intensity or shift of the O–H stretching peak (typically around 3,200 - 3,600 cm^{-1}) after nanoparticle synthesis indicates the involvement of hydroxyl groups in the reaction. A shift in the C=O stretching peak (typically observed around 1,650 - 1,750 cm^{-1}) or changes in its intensity suggests interaction between carbonyl groups and silver ions or nanoparticles [30]. The FTIR data indicate that the creation of silver nanoparticles was attributed to the O–H and C=O groups in the fingerroot extract, which functioned as stabilizing and reducing agents [31].

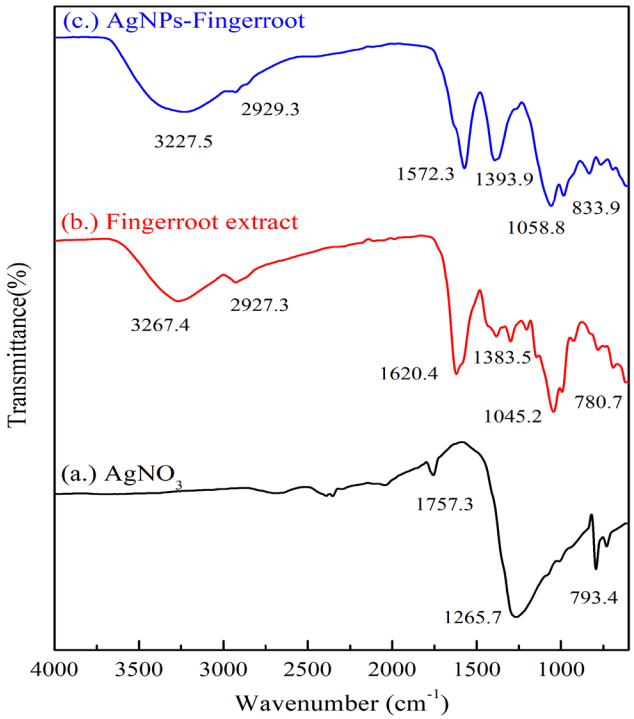

Figure 5 FT-IR spectra of the (a) $AgNO_3$ (b) Fingerroot extract, and (c) AgNP-fingerroot mixture.

***In situ* synthesis of AgNPs on muslin fabric fibers**

The muslin fabric was soaked *in situ* to synthesize AgNPs using fingerroot extract as a reducing agent. The results (**Figure 6**) related to the change in color indicated the adsorption of AgNPs on the surface of the textile fabric. The solution containing the textile fibers of muslin fabric turned from yellow (**Figure 6(a)**) to brown (**Figure 6(b)**). The color of the fabric changed from white to yellowish-brown. The appearance of a brown color confirmed the adsorption of AgNPs onto the fabric surface [32]. The fabric surface of muslin treated with AgNPs can enhance the antibacterial properties and UV light protection.

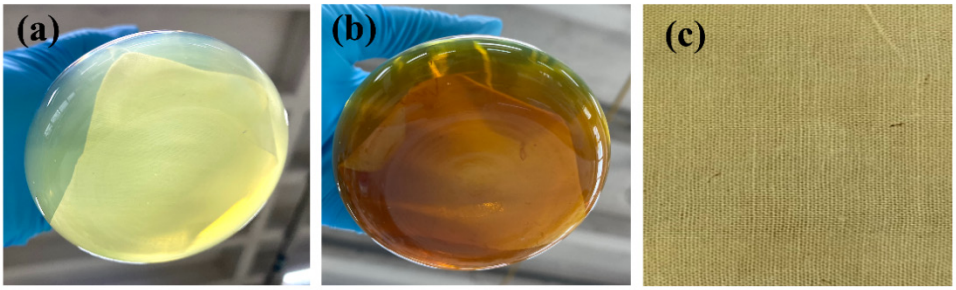

Figure 6 Color changes on the surface of textile fabric, with muslin (a) before being treated with AgNPs and (b) muslin after being treated with AgNPs. (c) Photographs of AgNP-treated muslin fabric.

The proposed mechanism of AgNP formation on muslin is described in **Figure 7**. The mechanism was derived from studies on the in situ green synthesis of AgNPs [33,34]. The biomolecules in the extract, such as flavonoids and polyphenols, control the generation and stability of AgNPs, independent of the green synthesis method used. First, the hydroxyl groups (–OH) of cellulose in the muslin react with the Ag^+ ions in the $AgNO_3$ precursor solution to produce nucleation sites for the nanoparticles. This reaction occurs when the muslin is immersed in the solution.

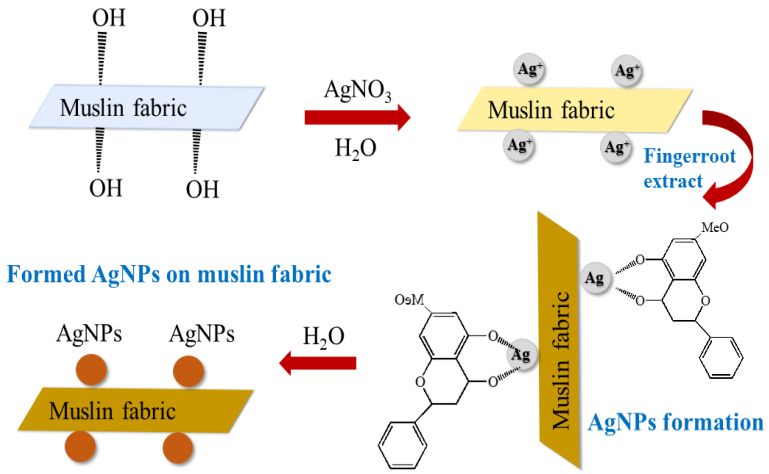

Figure 7 Schematic illustration of the formation of AgNPs on the surface of muslin fabrics by the fingerroot extract.

SEM/EDX analysis

The SEM micrograph of the untreated muslin fabric (**Figures 8(a) - 8(c)**) showed a smooth and clean surface. The SEM images of the muslin fabrics *in situ* treated with AgNP-fingerroot in **Figures 8(d) - 8(f)** showed the AgNP-fingerroot nanoparticles were coated on the muslin fibers. The adhesion of AgNPs to muslin fabric during washing was also examined. The distribution of AgNPs that remained adhered to the muslin fabric is shown in **Figures 8(g) - 8(i)**. The composition of the elements in the *in situ* AgNP-fingerroot-treated muslin fabric was confirmed via EDX spectroscopy, as illustrated in **Figure 9**. In the **Figure 9(a)** showed SEM mapping area of muslin fabric treated with AgNP-fingerroot. The untreated muslin fabric (**Figure 9(b)**) was found to contain 48.9 % oxygen (O) and 51.1 % carbon (C). However, the AgNP-fingerroot-coated muslin fabric had 48.9 % O, 49.8 % C, and 1.3 % silver (Ag). The strong silver signal observed at an energy level of 3.4 keV (**Figure 9(c)**) confirmed these findings [35]. After the AgNP-fingerroot-coated muslin fabric was washed with deionized water, the elemental composition slightly increased. These findings confirmed the presence and retention of the AgNP-fingerroot composite on the muslin fabric, indicating that it was stable and durable.

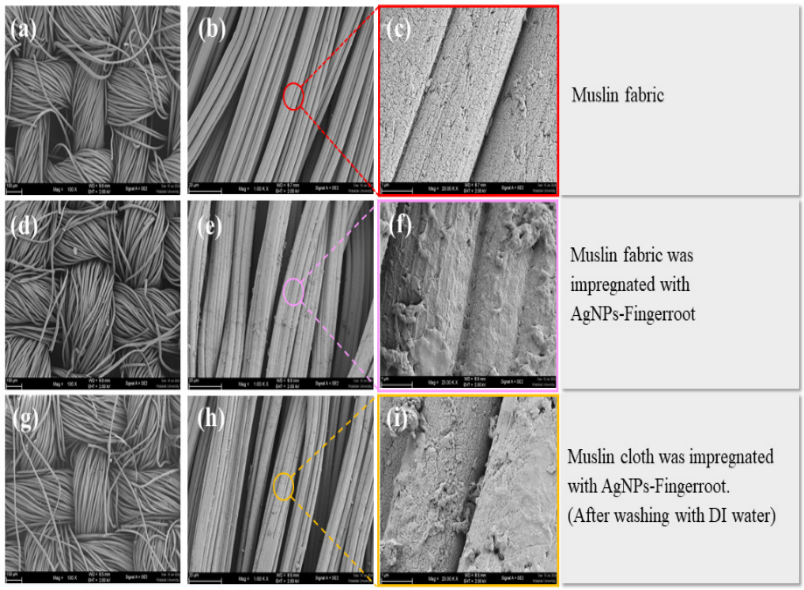

Figure 8 SEM images of different magnitudes of (a-c) untreated muslin fabric, (d-f) muslin fabric treated with AgNP-fingerroot, and (g-i) muslin fabric treated with AgNP-fingerroot after washing once with deionized water.

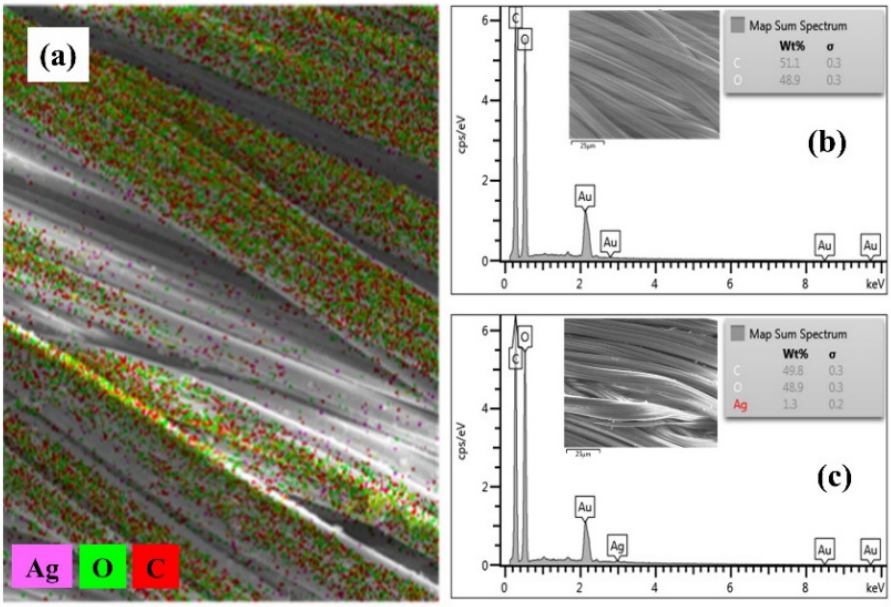

Figure 9 (a) SEM mapping area of muslin fabric treated with AgNP-fingerroot (b) EDX spectra of muslin fabric treated with AgNP-fingerroot, (c) EDX spectra of muslin fabric treated with AgNP-fingerroot after washing once with deionized water.

Antimicrobial activity

The antibacterial properties of the fingerroot extract, synthesized materials, and muslin fabric samples were evaluated by the agar-well diffusion method. The results of zone inhibition are presented in **Figure 10**. The untreated fabrics showed no evidence of an inhibition zone. In contrast, the fabrics treated with the synthesized AgNP-fingerroot displayed clear inhibition zones against *E. coli* and *S. aureus* were 8.5 ± 0.50 mm and 14.5 ± 0.50 mm in diameter, respectively. After the treated fabrics were washed once with deionized water, the inhibition zones decreased to 7.5 ± 0.50 mm and 12.5 ± 0.50 mm for *E. coli* and *S. aureus*, respectively. The untreated fabrics exhibited no antibacterial activity, whereas the treated muslin fabric maintained significant antibacterial properties even after being 10 wash cycles with deionized water, as determined by the presence of distinct inhibition zones. The findings of this study might be characterized as the mechanism: The generation of Reactive Oxygen Species (ROS) by AgNPs plays a key role in their antibacterial activity. ROS, including hydrogen peroxide, hydroxyl radicals, and superoxide anions, induce oxidative stress that breaks DNA strands, denatures proteins, and destroys bacterial membranes. Bacterial mortality results from the disruption of vital cellular activities caused by this multi-target mechanism. The generation of ROS and other effects, such as membrane rupture, guarantee that AgNPs are efficient against a variety of microorganisms [36]. This finding reflected the sustained antibacterial activity of the AgNP-fingerroot-treated fabric.

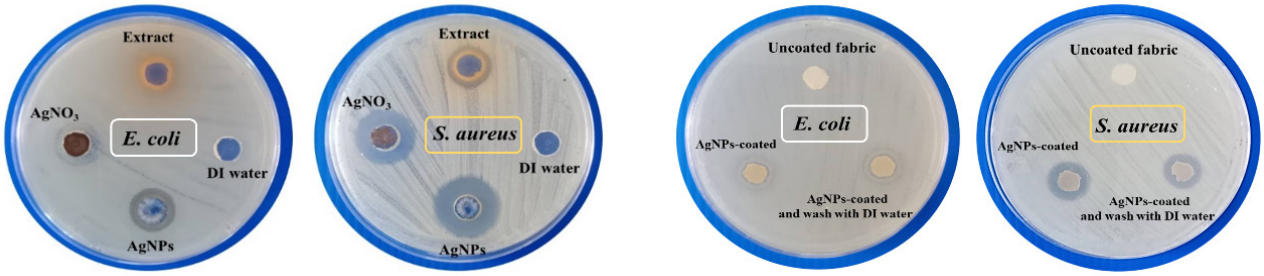

Figure 10 Antibacterial activities of untreated muslin cloth, treated muslin fabric, and treated muslin fabric after 10 wash cycles against *E. coli* and *S. aureus*.

UV protection analysis

the UV protection ability of the cotton fabric as determined by the UPF value. The UPF values for the untreated muslin fabric and AgNP-treated muslin fabric are presented in **Table 1**. The UV protection ability of the Untreated muslin fabric showed that it provided insufficient UV protection, with a UPF of only 6.42. The AgNP nanocomposite greatly increased the UV protection ability of the muslin fabric, as determined excellent protection by the UPF value of 43.30 referent from The UPF values and UV protection categories [37]. Besides, The natural material characteristics of the untreated muslin fabric result in inadequate UV protection. A lightweight cotton fabric with a loose weave, muslin has a porous structure that makes it easy for UV rays to penetrate. Natural cotton fibers are also inefficient at absorbing or dispersing UV rays because they lack inherent UV-blocking chemicals. The combination of compositional and structural elements causes untreated muslin cloth to have inadequate UV protection [38]. The UV protection ability of AgNP treated muslin after 10 wash cycles showed good protection with UV value of 18.22. These results because the nanoparticles could absorb and deflect UV light, improve the photostability and reflectivity of the muslin fabric, and promote stronger chemical connections that operate as efficient UV radiation barriers [39].

Table 1 UPF values for untreated and treated fabrics.

Samples	UPF value	Protection value
Untreated muslin fabric	6.42	Insufficient protection
AgNPs treated muslin fabric	43.30	Excellent protection
AgNPs treated muslin fabric After 10 wash clycles	18.22	good protection

Conclusions

This study revealed that fingerroot (*B. rotunda* (L.) Mansf.) extracts can be used as reducing agents for the in-situ synthesis of AgNPs on muslin fabric. The chemical composition of the extract promoted the formation of round AgNPs on muslin fabrics and imparted excellent protective properties to the cellulose fabrics against bacteria (*E. coli* and *S. aureus*) and UV radiation. The antimicrobial effects of the AgNP composite fingerroot against gram-positive *S. aureus* were stronger than those against gram-negative *E. coli*. Fingerroot extracts were found to reduce pinostrobin, attributed to the stability of the formed AgNPs, which showed good activity against *E. coli* and *S. aureus* and good UV protection of the muslin fabrics even after 10 wash cycles. The overall results are promising and provide a better understanding of the use of plant material for the green synthesis of AgNPs directly on cellulosic substrates. Future research we should focus on scalable, cost-effective production methods, such as standardized protocols and continuous flow reactors, to address scalability issues. Advanced binding techniques and protective coatings can minimize nanoparticle leaching and improve durability. Additionally, expanding treatment methods to various textiles and incorporating multifunctional properties can enhance the wider applicability of AgNP-coated fabrics.

Acknowledgements

The authors thank Materials Chemistry Research Center (MCRC), Department of Chemistry, Faculty of Science, and Center of Excellence for Innovation in Chemistry (PERCH-CIC), Khon Kaen University Consortium, Khon Kaen, Thailand for financial support. Special thanks the Fundamental Fund for academic year 2023 via KKU Research Affairs Division.

References

[1] X Han and X Gong. *In situ* one-pot method to prepare robust superamphiphobic cotton fabrics for high buoyancy and good antifouling. *ACS Applied Materials and Interfaces* 2021; **13(26)**, 31298-31309.

[2] X Zhang, P Li, Z Liu and H Wang and P Zhu. Eco-friendly multifunctional coating for polyester-cotton blended fabrics with superior flame retardancy and antibacterial

properties. *International Journal of Biological Macromolecules* 2024; **271(2)**, 132407.

[3] BW Hartanto and DS Mayasari. Environmentally friendly non-medical mask: An attempt to reduce the environmental impact from used masks during COVID 19 pandemic. *Science of the Total Environment*, 2021; **760(4)**, 144143.

[4] CM Clase, EL Fu, A Ashur, RC Beale, IA Clase, MB Dolovich, MJ Jardine, M Joseph, G Kansiime, JFE Mann, R Pecoits-Filho, WC Winkelmayer and JJ Carrero. Forgotten technology in the COVID-19 pandemic: Filtration properties of cloth and cloth masks-a narrative review. *Mayo Clinic Proceedings* 2020; **95(10)**, 2204-2224.

[5] M Rehan, HM Mashaly, MS Abdel-Aziz, RM Abdelhameed and AS Montaser. Viscose fibers decorated with silver nanoparticles via an in-situ green route: UV protection, antioxidant activities, antimicrobial properties, and sensing response. *Cellulose* 2024; **31**, 5899-5930.

[6] P Sundararajan and SP Ramasamy. Development of sustainable, eco-friendly antimicrobial finishing of cotton fabric using prodigiosin of *Serratia marcescens* SP1. *Progress in Organic Coatings* 2024; **188**, 108216.

[7] AV Mueller, MJ Eden, JM Oakes, C Bellini and LA Fernandez. Quantitative method for comparative assessment of particle removal efficiency of fabric masks as alternatives to standard surgical masks for PPE. *Matter* 2020; **3(3)**, 950-962.

[8] X Luo, Z Li, J Shen, L Liu, H Chen, Z Hu, I Krucinska and J Yao. A facile strategy to achieve efficient flame-retardant cotton fabric with durable and restorable fire resistance. *Chemical Engineering Journal* 2022; **430(3)**, 132854.

[9] N Rahmatian, S Abbasi, MT Yaraki and N Abbasi. *Echinophora platyloba* extract-mediated green synthesis of silver nanoparticles: Fine-tuning the size towards enhanced catalytic and antibacterial properties. *Journal of Molecular Liquids* 2023; **391(A)**, 123327.

[10] S Patel and N Patel. *Tectona grandis* seed mediated green synthesis of silver nanoparticles and their antibacterial activity. *Trends in Sciences*. 2023; **20(5)**, 5104.

[11] MM El-Zawahry, HS El-Khatib, GM Shokry and HG Rashad. One-pot robust dyeing of cotton fabrics with multifunctional chamomile flower dyes. *Fibers and Polymers* 2022; **23(8)**, 2234-2249.

[12] P Szczyglewska, A Feliczak-Guzik and I Nowak. Nanotechnology-general aspects: A chemical reduction approach to the synthesis of nanoparticles. *Molecules* 2023; **28(13)**, 4932.

[13] G Rajkumar and R Sundar. Sonochemical-assisted eco-friendly synthesis of silver nanoparticles (AgNPs) using avocado seed extract: Naked-eye selective colorimetric recognition of Hg^{2+} ions in aqueous medium. *Journal of Molecular Liquids* 2022; **368(A)**, 120638.

[14] S Anis, WC Liew, AM Marsin, II Muhamad, SH Teh and AZM Khudzari. Microwave-assisted green synthesis of silver nanoparticles using pineapple leaves waste. *Cleaner Engineering and Technology* 2023; **15(1)**, 100660.

[15] MMI Masum, MM Siddiqa, KA Ali, Y Zhang, Y Abdallah, E Ibrahim and B Li. Biogenic synthesis of silver nanoparticles using *Phyllanthus emblica* fruit extract and its inhibitory action against the pathogen *Acidovorax oryzae* strain RS-2 of rice bacterial brown stripe. *Frontiers in microbiology* 2019; **10**, 820.

[16] Hemlata, PR Meena, AP Singh and KK Tejavath. Biosynthesis of silver nanoparticles using *Cucumis prophetarum* aqueous leaf extract and their antibacterial and antiproliferative activity against cancer cell lines. *ACS omega* 2020; **5(10)**, 5520-5528.

[17] P Porrawatkul, R Pimsen, A Kuyyogsuy, N Teppaya, A Noypha, S Chanthai and P Nuengmatcha. Microwave-assisted synthesis of Ag/ZnO nanoparticles using *Averrhoa carambola* fruit extract as the reducing agent and their application in cotton fabrics with antibacterial and UV-protection properties. *RSC Advances* 2022; **12(24)**, 15008-15019.

[18] Z Zulfiqar, R Rashad, M Khan, M Summer, Z Saeed, M Pervaiz, S Rasheed, B Shehzad, F Kabir and S Ishaq. Plant-mediated green synthesis of silver nanoparticles: Synthesis, characterization, biological applications, and toxicological considerations: A review. *Biocatalysis and Agricultural Biotechnology*, 2024; **57**, (103121).

[19] NQ Hop and NT Son. *Boesenbergia rotunda* (L.) Mansf.: A review of phytochemistry, pharmacology, and pharmacokinetics. *Current Organic Chemistry* 2023, **27(21)**, 1842-1856.

[20] L Suhaimi, E Dwi, S Bahtiar, R Desiasni, F Widyawati and S Ali. Biosynthesis and characterization of micro structured zinc oxide (ZnO) thin films using fingerroot (*Boesenbergia rotunda*) extract by dip coating technique. *AIP Conference Proceedings* 2024; **3026**, 030003.

[21] P Wongwitthayakool and M Pudla. Thermal properties of acrylic resin denture base material containing silver nanoparticle synthesized from aqueous extract of *Boesenbergia rotunda*. *Key Engineering Materials* 2018; **777**, 173-177.

[22] A Kara and B Ozcelik. Green synthesis of chitosan-coated silver nanoparticles (ch-agnps): harnessing nature for sustainable and safe nanomaterial production. *Journal of The Institute of Science and Technology* 2024; **7(3)**, 1319-1341.

[23] JU Kim, MS Gong and JG Kim. Preparation of Ag/ZnO-coated cotton fabrics with UV blocking and antibacterials properties. *Cellulose Chemistry and Technology* 2018; **52(5-6)**, 475-484.

[24] HT San, HEF Khine, B Sritularak, E Prompetchara, C Chaotham, CT Che and K Likhitwitayawuid. Pinostrobin: An adipogenic suppressor from fingerroot (*Boesenbergia rotunda*) and its possible mechanisms. *Foods* 2022; **11(19)**, 3024.

[25] V Maduraimuthu, JK Ranishree, RM Gopalakrishnan, B Ayyadurai, R Raja and K Heese. Antioxidant activities of photoinduced phycogenic silver nanoparticles and their potential applications. *Antioxidants* 2023; **12(6)**, 1298.

[26] M Nakhjavani, V Nikkhah, MM Sarafraz, S Shoja and M Sarafraz. Green synthesis of silver nanoparticles using green tea leaves: Experimental study on the morphological, rheological and antibacterial behaviour. *Heat and Mass Transfer* 2017; **53(10)**, 3201-3209.

[27] BH Rathod, SS Rani, N Kartheek and AA Kumar. UV spectrophotometric method development and validation for the quantitative estimation of indinavir sulphate in capsules. *International Journal of Pharmacy and Pharmaceutical Sciences* 2014; **6(6)**, 598-601.

[28] YM Kim, M Lubinska-Szczygeł, YS Park, J Deutsch, A Ezra, P Luksrikul, RMB Shafreen and S Gorinstein. Characterization of bioactivity of selective molecules in fruit wines by FTIR and NMR spectroscopies, fluorescence and docking calculations. *Molecules* 2023; **28(16)**, 6036.

[29] NJ Elahi, S Masoud, T Danial, H Alireza and D Majid. Ammonia sensing and cytotoxicity of the biosynthesized silver nanoparticle by Arabic gum (AG). *Recent Patents on Biotechnology* 2019; **13(3)**, 228-238.

[30] HR El-Seedi, MS Omara, AH Omar, MM Elakshar, YM Shoukhba, H Duman, S Karav, AK Rashwan, AH El-Seedi, HA Altaleb, H Gao, A Saeed, OA Jefri, Z Guo and SAM Khalifa. Updated review of metal nanoparticles fabricated by green chemistry using natural extracts: Biosynthesis, mechanisms, and applications. *Bioengineering* 2024; **11(11)**, 1095.

[31] K Seku, SS Hussaini, M Hussain, MA Siddiqui, N Golla, R Dachepalli and B Reddy. Synthesis of Frankincense gum stabilized AgNPs by microwave irradiation and their catalytic, antioxidant, and antibacterial properties. *Physica E: Low-Dimensional Systems and Nanostructures* 2022; **140(1)**, 115169.

[32] P Tooklang, S Audtarat, K Chaisen, J Thepsiri, A Chingsungnoen, P Jittabut and T Dasri. Functionalization of silver nanoparticles coating cotton fabrics through hydrothermal synthesis for improved antimicrobial properties. *Nano Express* 2024; **5(2)**, 025009.

[33] SS Dash, S Samanta, S Dey, B Giri and SK Dash. Rapid green synthesis of biogenic silver nanoparticles using *Cinnamomum tamala* leaf extract and its potential antimicrobial application against clinically isolated multidrug-resistant bacterial strains. *Biological Trace Element Research* 2020; **198**, 681-696.

[34] P Sivaranjana, ER Nagarajan, N Rajini, N Ayrilmis, AV Rajulu and S Siengchin. Preparation and characterization studies of modified cellulosic textile fabric composite with in situ-generated AgNPs coating. *Journal of Industrial Textiles* 2021; **50(7)**, 1111-1126.

[35] AH Labulo, OA Davi and AD Terna. Green synthesis and characterization of silver

nanoparticles using Morinda lucida leaf extract and evaluation of its antioxidant and antimicrobial activity. *Chemical Papers* 2022; **76(12)**, 7313-7325.

[36] PR More, S Pandit, AD Filippis, G Franci, I Mijakovic and M Galdiero. Silver nanoparticles: Bactericidal and mechanistic approach against drug resistant pathogens. *Microorganisms* 2023; **11(2)**, 369.

[37] TS Kim, JR Cha and MS Gong. Investigation of the antimicrobial and wound healing properties of silver nanoparticle-loaded cotton prepared using silver carbamate. *Textile Research Journal* 2018; **88(7)**, 766-776.

[38] OK Alebeid and T Zhao. Review on: Developing UV protection for cotton fabric. *The Journal of the Textile Institute* 2017, **108(12)**, 2027-2039.

[39] N Chen, CK Liu, EM Brown and N Latona. Environment-friendly treatment to reduce photoyellowing and improve UV-blocking of wool. *Polymer Degradation and Stability* 2020; **181**, 109319.